Supplementary Information

Bend, Don't Break: Exploring the Mechanochromic, AIE and Non-Linear Optical Properties of Carbazole-Thiobarbituric Acid Hybrids.

Meema Rasheed,[a] R Lakshmi,[b] Parvathy O.C.,[a] Shandev P.P.,[a] Pramod Gopinath,*[b, c]

Narayanapillai Manoj,*[a, c]

[a] *Department of Applied Chemistry, Cochin University of Science and Technology, Kochi 682022, Kerala, India*

[b] *International School of Photonics, Cochin University of Science and Technology, Kochi 682022, Kerala, India*

[c] *Inter University Centre for Nanomaterials and Devices, Cochin University of Science and Technology, Kochi-682022, Kerala, India*

E-mail: manoj.n@cusat.ac.in, pramod@cusat.ac.in

Table of Contents

1. Experimental Procedures

Synthesis of 5-((9-alkyl-9H-carbazol-3-yl) methylene)-2-thioxodihydropyrimidine-4,6(1H,5H)-dione_(TBA conjugate)

N-alkylcarbazole-thiobarbituric acid conjugates were synthesized via Knoevenagel condensation.[1] 9-alkyl-9H-carbazole-3-carbaldehyde (1 eqv.) and thiobarbituric acid (1 eqv.) were reacted in ethanol at 60°C for 5 hours. The resulting precipitated TBA conjugate was filtered, washed with hot water, and dried under vacuum. The reaction yielded 80% of the desired product.

2. Results and discussion

Characterisation of TBA conjugates

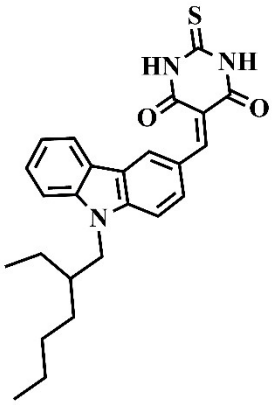

ETBA: m.p. > 250 °C, FT-IR (KBr, ν_{max} cm^{-1}): 3436, 3140, 2352, 1642, 1533. **^{1}H NMR** (400 MHz, $CDCl_3$, δ ppm) 0.85 (t, 3H), 0.92 (t, 3H), 1.22 – 1.42 (m, 9H), 4.2 (d, 2H), 7.30 – 7.46 (m, 4H), 7.50 – 7.56 (m, 1H), 8.37 (d, 1H), 8.59 (d, 1H), 8.76 (s, 1H), 8.93 (d, 1H), 9.36 (s, 1H). **MALDI-TOF MS** (ESI MS) m/z: $[M+H]^+$ calcd for $C_{25}H_{27}N_3O_2S$ 434.1902, found 434.9803.

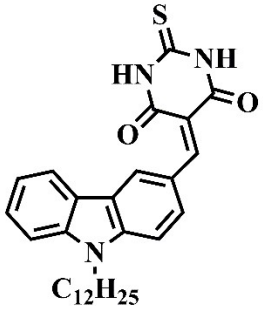

DTBA: m.p. >250 °C, **FT-IR** (KBr, ν_{max} cm^{-1}): 3426, 3120, 2362, 1646, 1533. **^{1}H NMR** (400 MHz, DMSO-d_6, δ ppm) 0.83 (t, 3H), 1.16 – 1.26 (m, 18H), 1.78 – 1.84 (m, 2H), 4.48 (t, 2H), 7.34 (t, 1H), 7.55 (t, 1H), 8.21 (d, 1H), 8.56 (s, 1H), 8.66 – 8.68 (m, 1H), 9.36 (s, 1H), 12.29 (s, 1H), 12.38 (s, 1H). **MALDI-TOF MS** (ESI MS) m/z: $[M+H]^+$ calcd for $C_{29}H_{36}N_3O_2S$ 490.2523, found 490.7923.

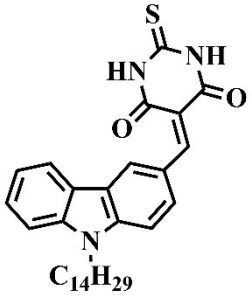

TTBA: m.p. > 250 °C, FT-IR (KBr, ν_{max} cm^{-1}): 3420, 3156, 2350, 1654, 1517. **^{1}H NMR** (400 MHz, $CDCl_3$, δ ppm) 0.86 (t, 3H), 1.22 – 1.41 (m, 20H), 1.71 (s, 2H), 1.89 (t, 2H), 4.33 (t, 2H), 7.38 (m, 1H), 7.43 – 7.46 (m, 2H), 7.51 – 7.56 (m, 1H), 8.27 (d, 1H), 8.58 (d, 1H), 8.76 (s, 1H), 8.90 (d, 2H), 9.37 (s, 1H). **MALDI-TOF MS** (ESI MS) m/z: $[M+H]^+$ calcd for $C_{31}H_{39}N_3O_2S$ 518.2841, found 518.5560

Global-Reactivity Parameters

Valuable theoretical understanding of chemical reactivity and selectivity parameters by examining fundamental qualitative chemical concepts such as ionisation potential (IP), electron affinity (EA), electronegativity (χ), chemical potential (μ), global hardness (η), softness (σ), and electrophilicity index (ω). Molecules with higher chemical potential (μ) and hardness (η) values are considered to be kinetically stable. These parameters are directly associated with orbital Egap values and are inversely correlated with overall softness (σ). Additionally, GRPs can be calculated using equations 1 and 2.

$$IP = -E_{HOMO} \quad (1)$$

$$EA = -E_{LUMO} \quad (2)$$

IP and EA are the ionisation potential and electron affinity (in a.u.). Electronegativity (χ), chemical hardness (η), and chemical potential (μ) have been determined using the Koopmans theorem with equations 3-5.

$$\chi = \frac{[IP + EA]}{2} = -\frac{[E_{LUMO} + E_{HOMO}]}{2} \quad (3)$$

$$\eta = \frac{[IP - EA]}{2} = -\frac{[E_{LUMO} - E_{HOMO}]}{2} \quad (4)$$

$$\mu = \frac{E_{HOMO} + E_{LUMO}}{2} \quad (5)$$

Equations 6 and 7 give the global softness (σ) and electrophilicity index (ω)

$$\sigma = \frac{1}{2\eta} \quad (6)$$

$$\omega = \frac{\mu^2}{2\eta} \quad (7)$$

	IP	**EA**	χ	η	μ	σ	ω
ETBA	0.2235	0.1054	0.1644	0.0590	-0.1644	8.4745	0.2290
DTBA	0.2234	0.1051	0.1642	0.0591	-0.1642	8.4602	0.2281
TTBA	0.2233	0.1051	0.1642	0.0591	-0.1642	8.4602	0.2281

Table 1. Global reactivity parameters of ETBA, DTBA and TTBA.

Theoretical calculations

Previous research revealed the similar molecule's twisted intramolecular charge transfer (TICT) state.[2] This conclusion was based on Lippert-Mataga analysis and excited-state DFT calculations. The presence of a TICT state explains the observed red shift in emission spectra in polar solvents.

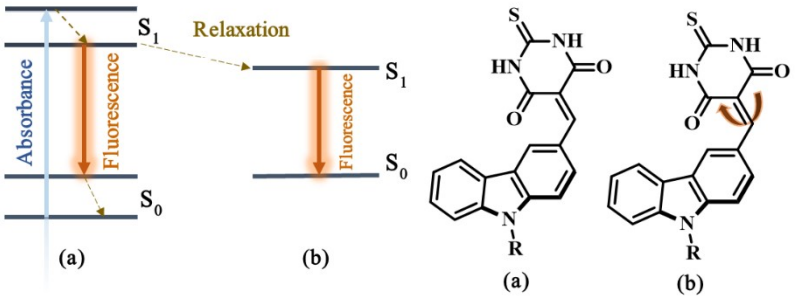

Fig. 1 Diagram showing emission in TICT state of TBA conjugates in (a) Planar and (b) when excited, these molecules can twist, leading to a unique emission profile.

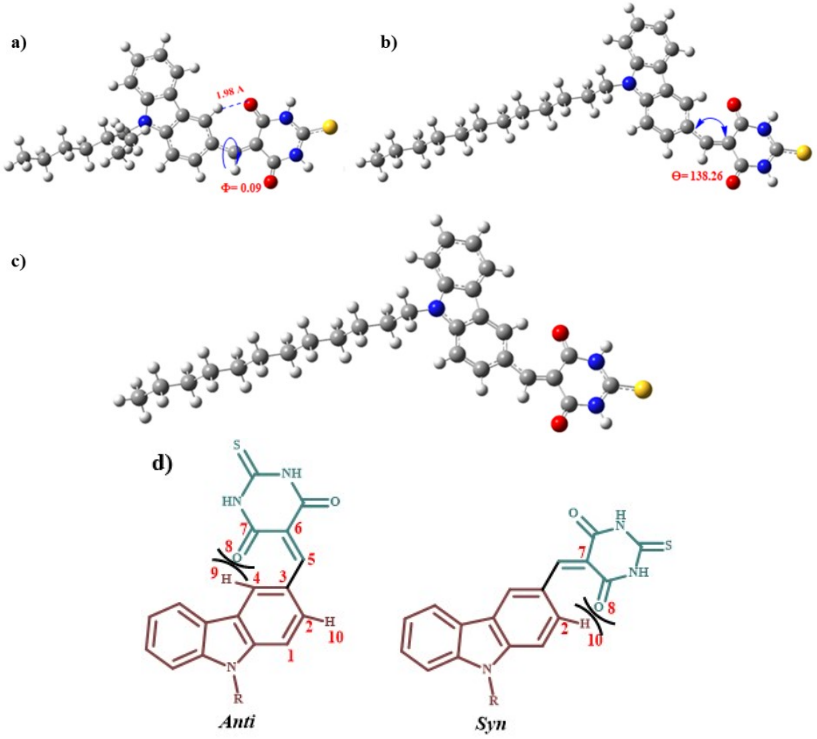

Chart. 1 Optimized ground state geometry of a) ETBA, b) DTBA, c) TTBA in gaseous state, d) *Anti* and *Syn* conformations of TBA conjugates

Non-Linear Optical property

Theoretical evaluation

To understand how TBA conjugates behave optically in water and THF, we used DFT methods with B3LYP and a 6-311++G(d,p) basis set to calculate their static dipole moment (μ_{total}), total polarizability (α_{tot}), polarizability anisotropy ($\Delta\alpha$), static first-order hyperpolarizability (β_{total}), and second-order hyperpolarizability (γ). We assumed the molecules are in a static external electric field F, and their energy is expressed as the function of the static field F,[3] as shown in equation 8.

$$E(F) = E(0) - \mu_i F_i - \frac{1}{2}\alpha_{ij} F_i F_j - \frac{1}{6}\beta_{ijk} F_i F_j F_k - \frac{1}{24}\gamma_{ijkl} F_i F_j F_k F_l \quad (8)$$

The total static dipole moment (μ_{tot}) is determined by using this equation[4,5]: $\mu_{tot} = \sum \mu i$

$$\mu_i = (\mu_{x^2} + \mu_{y^2} + \mu_{z^2})^{1/2} \quad (9)$$

A second-rank tensor describes the polarizability; the mean or total polarizability (αtot) can be determined by solely considering the diagonal elements, as follows: [4,5]

$$\alpha_{ij} = \frac{(\alpha_{xx} + \alpha_{yy} + \alpha_{zz})}{3} \quad (10)$$

The anisotropy of the polarizability Δα can be expressed as [6,7]

$$\Delta\alpha = \frac{1}{\sqrt{2}}\sqrt{[(\alpha_{xx} - \alpha_{yy})^2 + (\alpha_{yy} - \alpha_{zz})^2 + (\alpha_{zz} - \alpha_{xx})^2 + 6(\alpha^2{}_{xy} + \alpha^2{}_{yz} + \alpha^2{}_{xz}]} \quad (11)$$

A third-rank tensor represents the static first-order hyperpolarizability (βtot). The 27 components of the 3D matrix can be reduced to 10 elements by Kleinman symmetry.[8] The output file from Gaussian 03W provides the following main components: β_{xxx}, β_{xxy}, β_{xyy}, β_{yyy}, β_{xxz}, β_{xyz}, β_{yyz}, β_{xzz}, β_{yzz}, β_{zzz}. The first hyperpolarizability (β_{tot}) is defined as equation 12.[6,9]

$$\beta_{ijk} = \sqrt{(\beta_{xxx} + \beta_{xyy} + \beta_{xzz})^2 + (\beta_{xxy} + \beta_{yyy} + \beta_{yzz})^2 + (\beta_{xxz} + \beta_{zyy} + \beta_{zzz})^2} \quad (12)$$

The average value of the static hyperpolarizability of the second order (γ_{tot}) is given by equation 13,[10]

$$\gamma_{ijk} = \frac{1}{5}[\gamma_{xxxx} + \gamma_{yyyy} + \gamma_{zzzz} + 2(\gamma_{xxyy} + \gamma_{yyzz} + \gamma_{xxzz})] \quad (13)$$

Organic molecules with NLO behaviour are believed to result from strong ICT character, which allows for the transfer of electron density from donor to acceptor along a π bridge.[11] The organic molecule urea is commonly used as a reference material for comparing NLO properties. The β_{tot} value for urea is 37.28 x 10^{-32} esu,[12] while the β_{tot} values for our synthesised D-π-A conjugates are notably higher. This indicates that ETBA, DTBA, and TTBA are favourable candidates for NLO applications. ETBA exhibits high values of β_{tot} and γ in water and THF due to its strong ICT character,[13] leading to enhanced nonlinearity compared to other D-π-A conjugates.

UV-Visible absorption properties

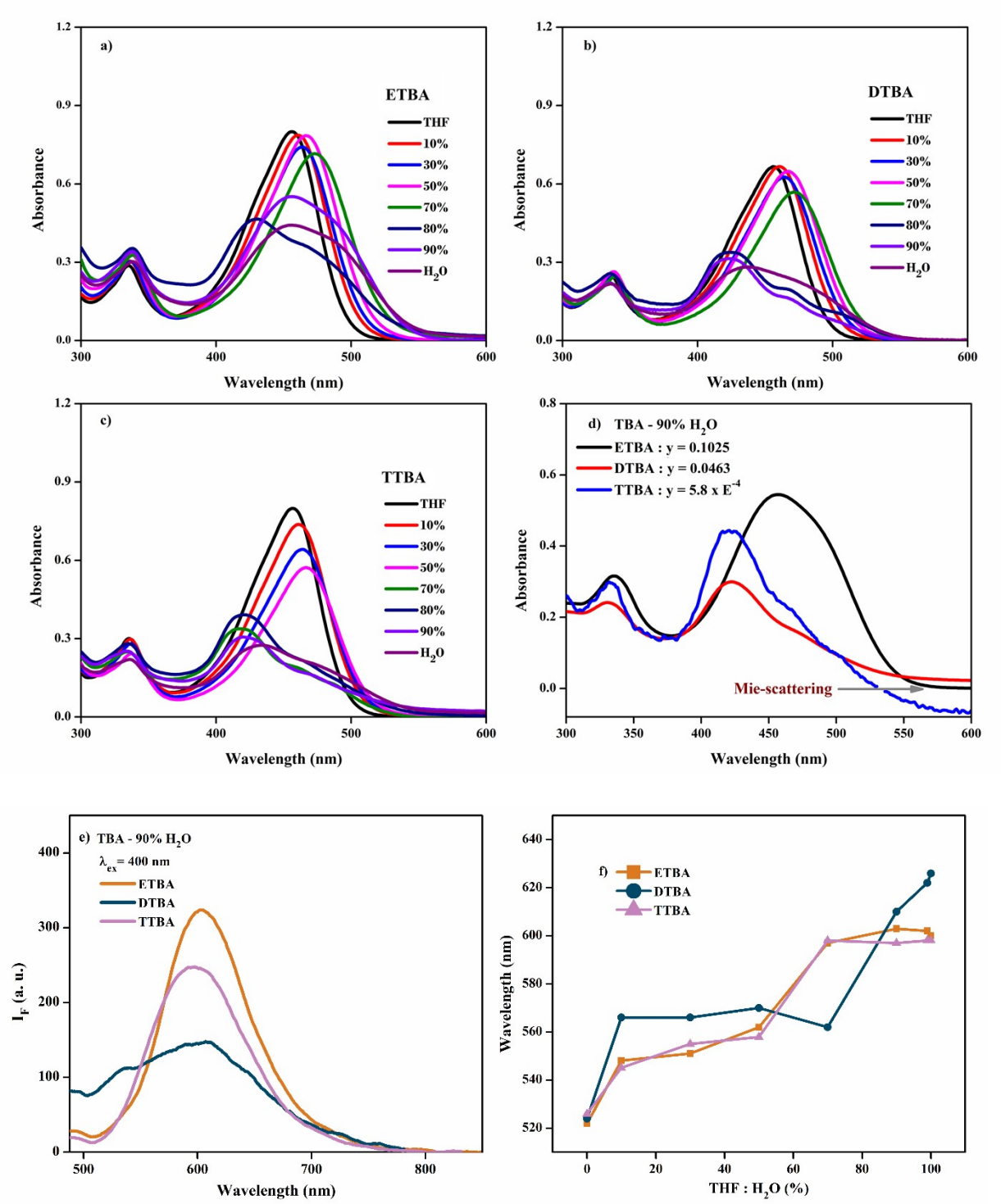

Fig. 2 Absorption spectra of (a) ETBA, (b) DTBA, (c) TTBA in (2×10^{-3} M) THF: H_2O ratios, (d) TBA conjugates in *fw*= 90% and emission spectra, (e) at *fw*= 90%, (f) plot of λ_{max} vs. THF: H_2O (%) ratios.

Morphology studies of TBA conjugates

Fig. 3 shows the TEM morphology image of the TBA conjugates, where nanorods having uniform diameters with flat and smooth surfaces were seen in ETBA (a,b) and TTBA (e,f). In DTBA (c,d), a sheet-like structure that winds up to form a fibre bundle was observed.

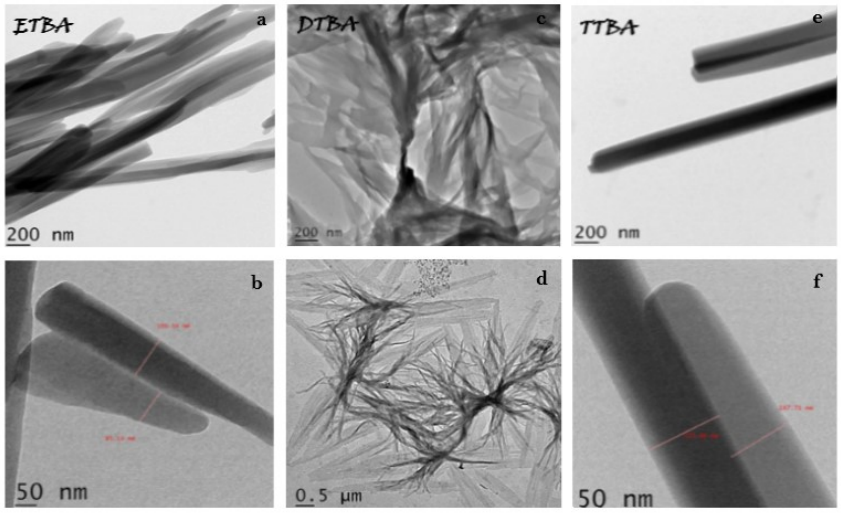

Fig. 3 TEM images of the self-assembled structures of **ETBA** (a, b), **DTBA** (c,d), and **TTBA** (e,f).

Aggregate size Measurement

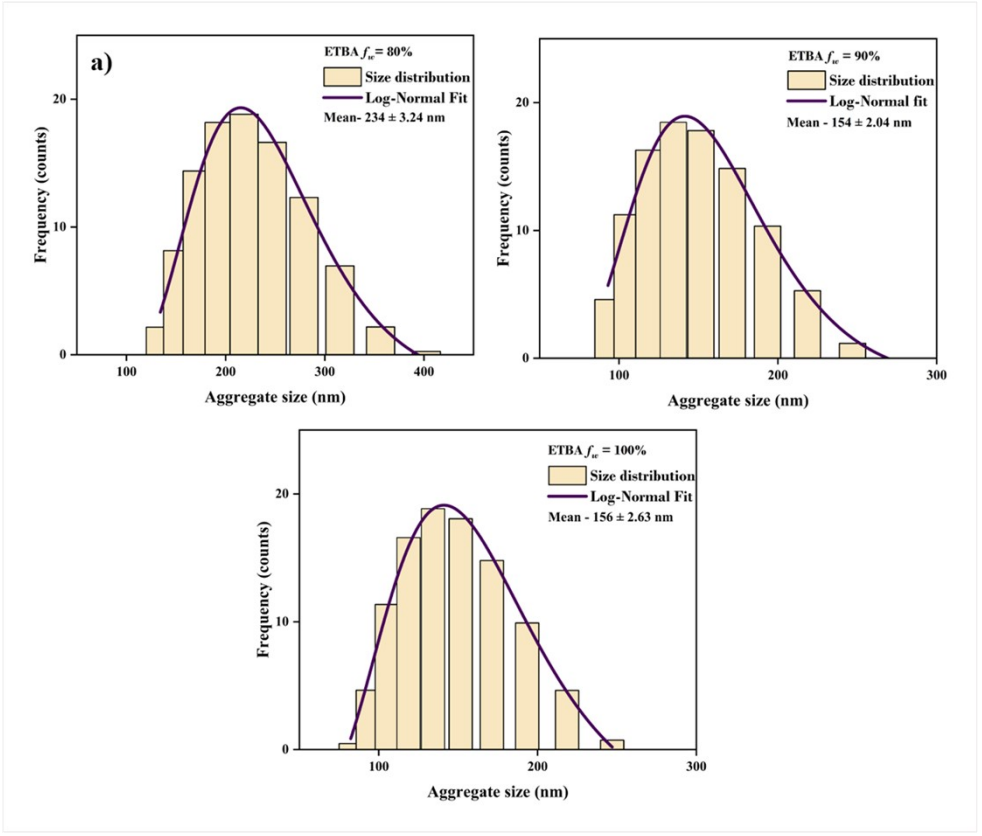
a)
ETBA f_{se} = 80%
Size distribution
Log-Normal Fit
Mean- 234 ± 3.24 nm
ETBA f_{se} = 90%
Size distribution
Log-Normal fit
Mean - 154 ± 2.04 nm
ETBA f_{se} = 100%
Size distribution
Log-Normal Fit
Mean - 156 ± 2.63 nm
Frequency (counts)
Aggregate size (nm)

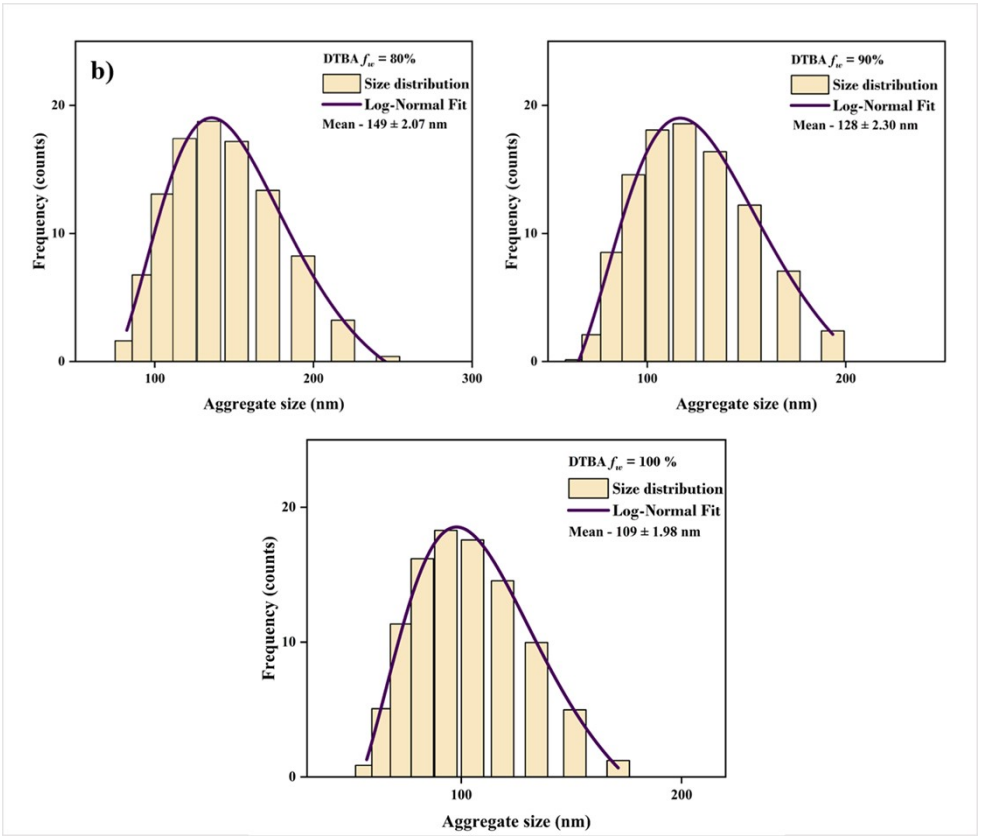
b)
DTBA f_{se} = 80%
Size distribution
Log-Normal Fit
Mean - 149 ± 2.07 nm
DTBA f_{se} = 90%
Size distribution
Log-Normal Fit
Mean - 128 ± 2.30 nm
DTBA f_{se} = 100 %
Size distribution
Log-Normal Fit
Mean - 109 ± 1.98 nm
Frequency (counts)
Aggregate size (nm)

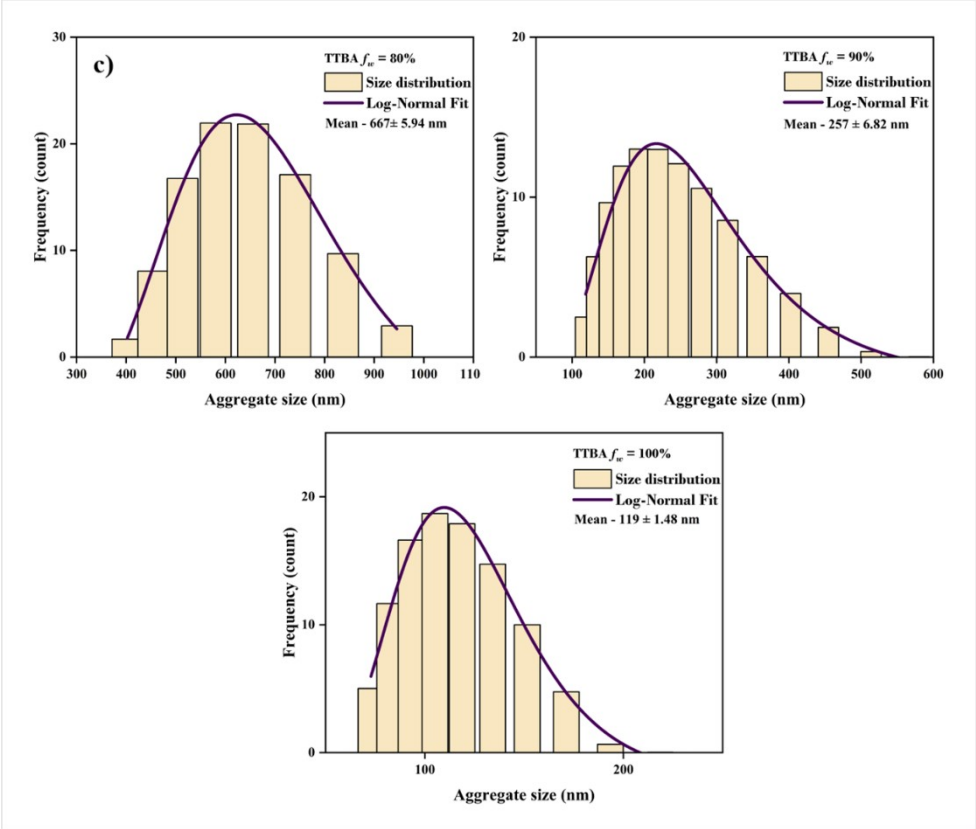

Fig. 4 Particle size histograms obtained from the DLS analysis for (**a**) ETBA, (**b**) DTBA and (**c**) TTBA, at *fw*=80%, 90% and 100% and the fits of the data according to a log-normal distribution (Concentration: 2×10^{-3} mol/L).

Mechanofluorochromic properties

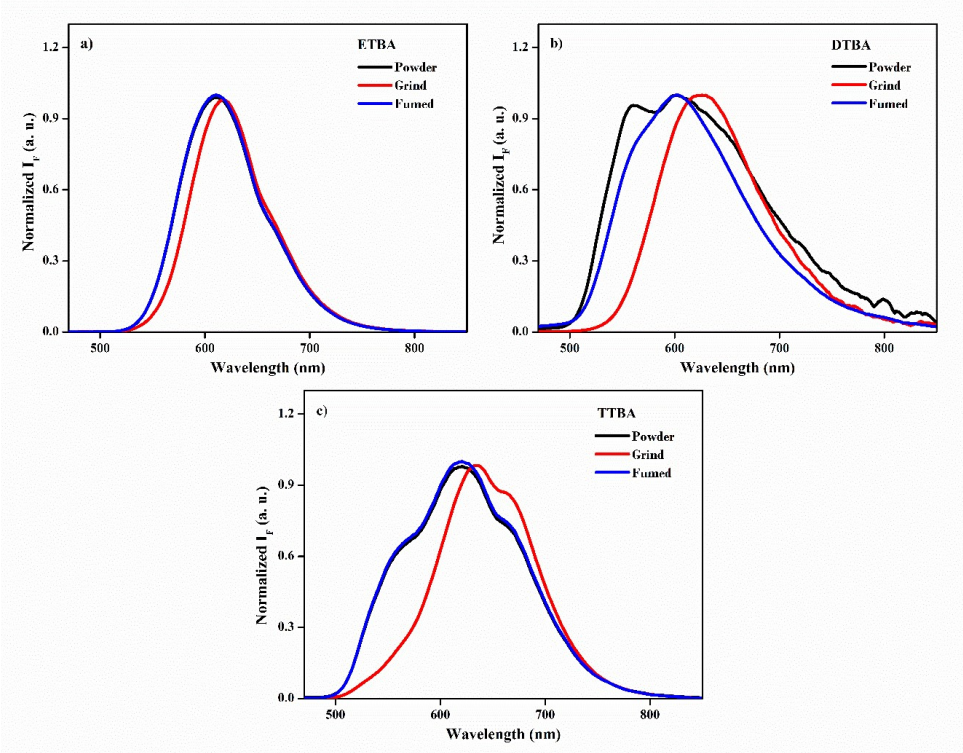

Fig. 5 Normalized emission spectra (λex = 450 nm) of TBA Conjugates under external stimuli, showing the grinding-induced spectral shift ($\Delta\lambda$).

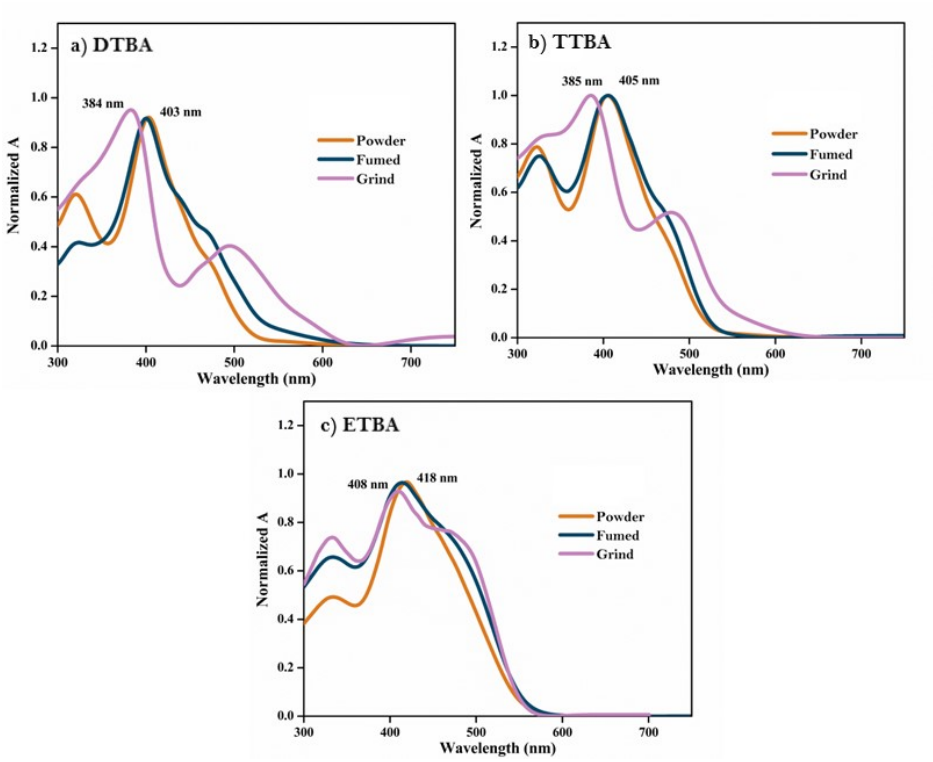

Fig. 5.1 UV-DRS spectra of TBA Conjugates under external stimuli, showing the grinding-induced spectral shift ($\Delta\lambda$).

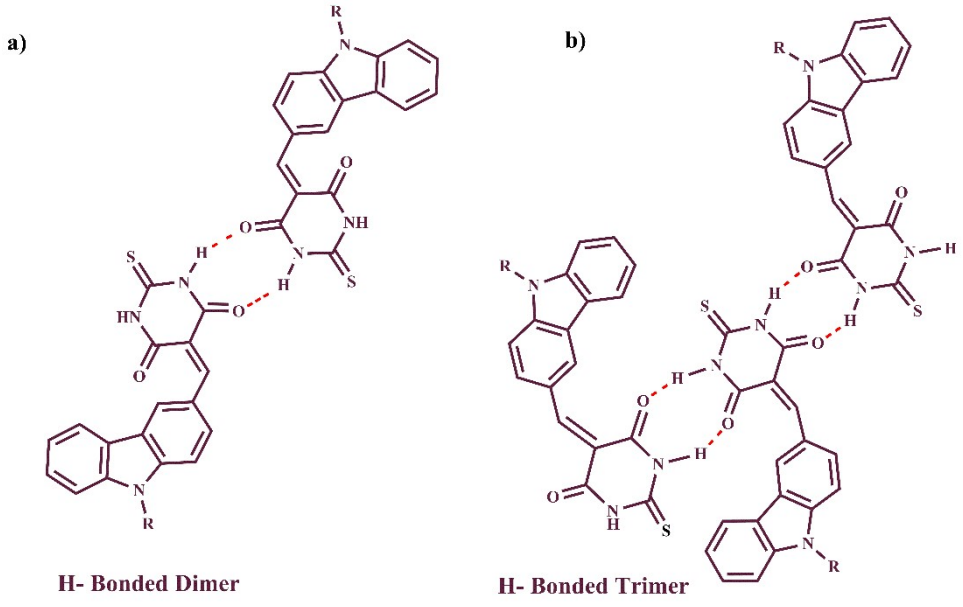

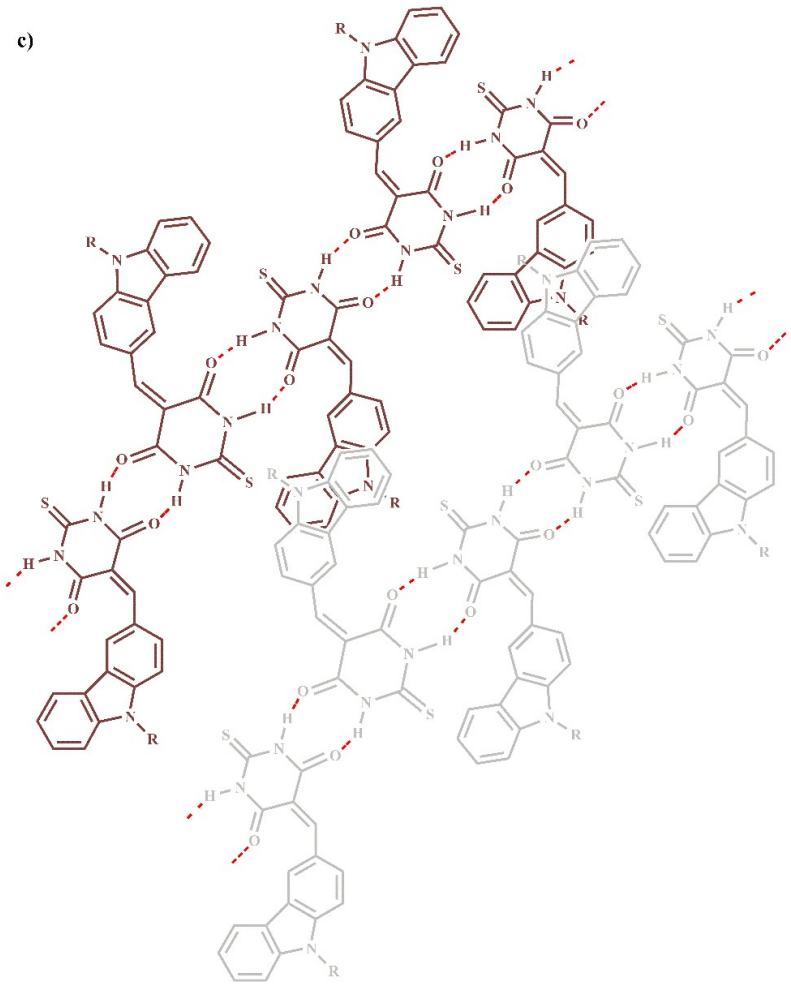

Scheme 2. Hydrogen-bonded dimers and trimers of TBA conjugates. H-bonding, π-stacking, and hydrophobic association assisted hierarchical assemblies of TBA conjugates in solution.

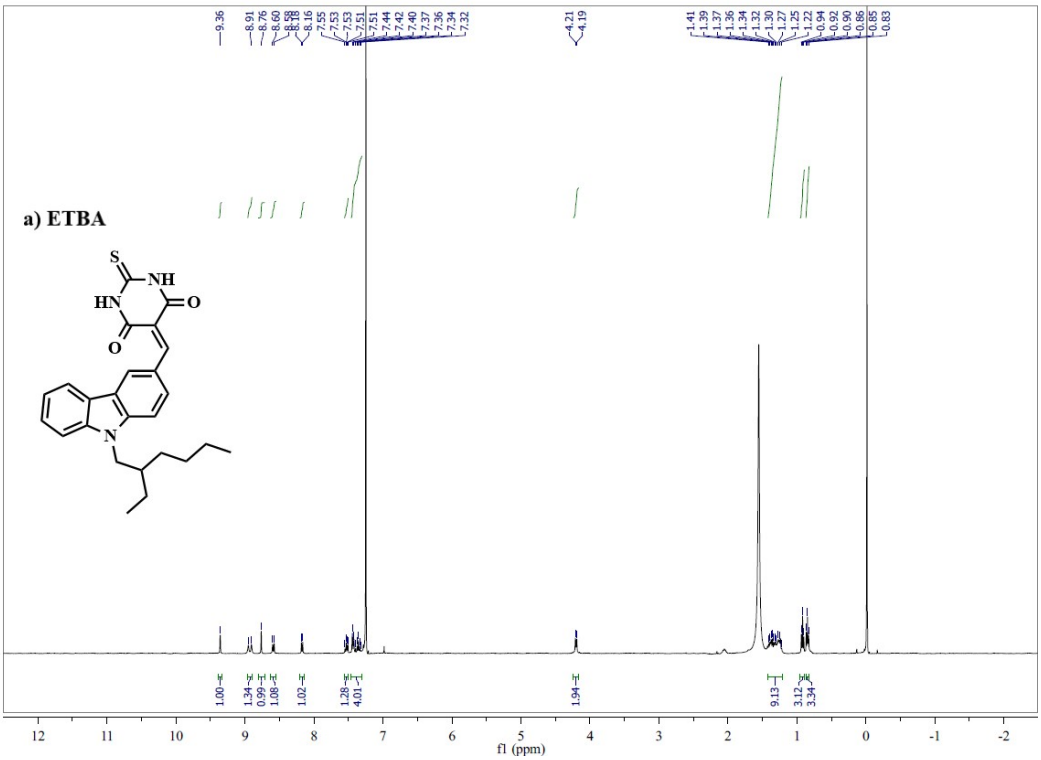
a) ETBA
f1 (ppm)

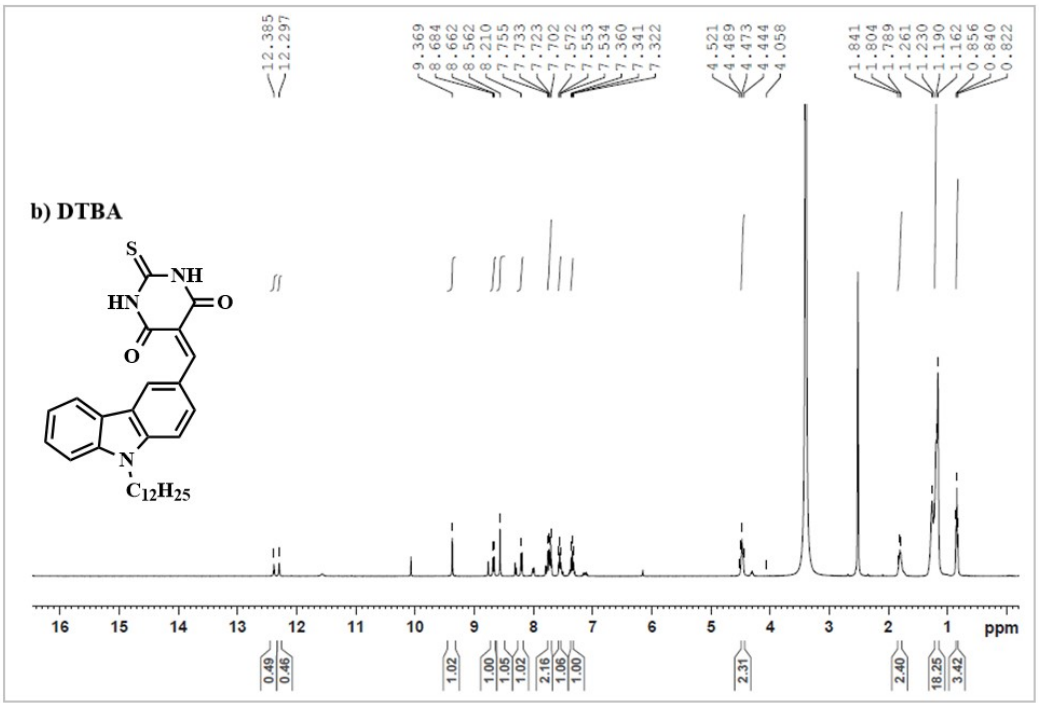
b) DTBA
C12H25
ppm

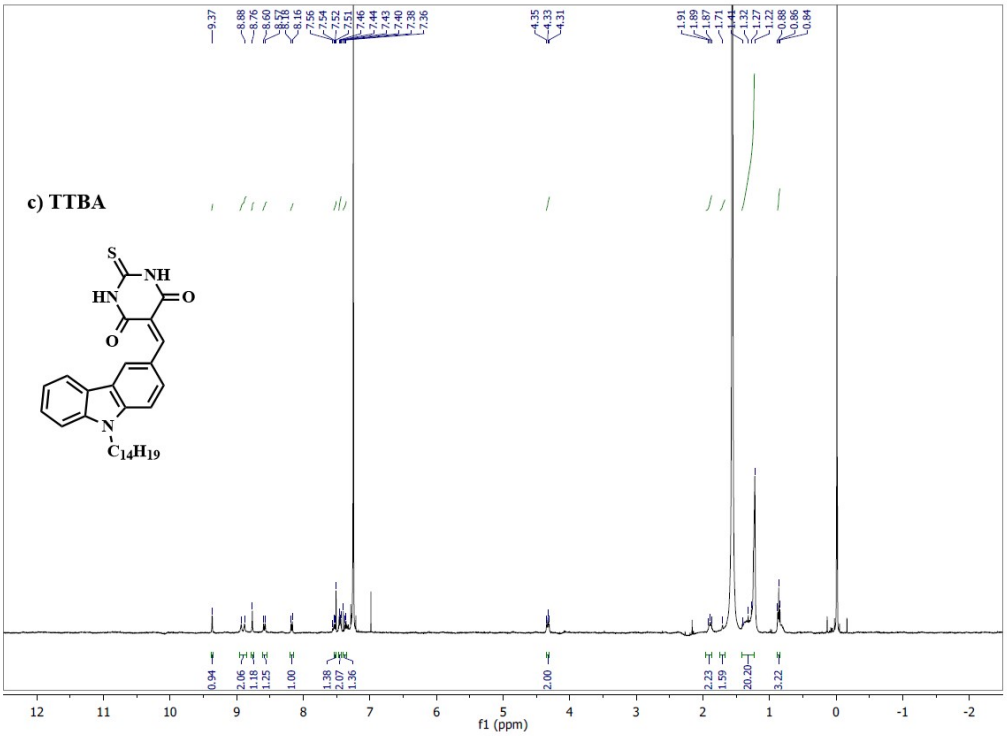

Fig. 6 1H-NMR spectra of a) ETBA, c) TTBA IN $CDCl_3$ and b) DTBA in DMSO at 400 MHz.

References

1. K. Kala, P. K. Vineetha and N. Manoj, *New J. Chem*., 2017, 41, 5176–5181.

2. Kala, K. *Ph. D. Thesis*, *CUSAT*. **2016**

3. S. Udayan, A.C. Kuriakose, P. Mary, D. Sherin, T. Manojkumar, V. Nampoori and S. Thomas, *Spectrochim. Acta Part A Mol. Biomol. Spectrosc.*, 2022, 272, 121011.

4. N. Sundaraganesan, J. Karpagam, S. Sebastian and J. P. Cornard, *Spectrochim. Acta Part A: Mol. Biomol. Spectrosc.*, 2009, 73, 11–19.

5. R. Zhang, B. Du, G. Sun and Y. Sun, *Spectrochim. Acta Part A: Mol. Biomol. Spectrosc.*, 2010, 75, 1115–1124.

6. N. Islam and I. H. Lone, *Front. Chem.*, 2017, 5, 11.

7. D. S. Sabirov, *RSC Adv.*, 2014, 4, 44996–45028.

8. S. Cabuk, *Cent. Eur. J. Phys.*, 2012, 10, 239–252.

9. K. S. Thanthiriwatte and K. N. De Silva, *J. Mol. Struct. THEOCHEM*, 2002, 617, 169–175.

10. H. A. Kurtz, J. J. Stewart and K. M. Dieter, *J. Comput. Chem.*, 1990, 11, 82–87.

11. M. U. Khan, M. Ibrahim, M. Khalid, A.A.C. Braga, S. Ahmed and A. Sultan, *J. Clust. Sci.*, 2019, 30, 415–430.

12. B. Raaghul, M.R. Kannan and T. Vijayakumar, *IOP Conf. Ser. Mater. Sci. Eng.*, 2022, 1219, 012035.

13. P.K. Vineetha, A. Aswathy, E. Shiju, K. Chandrasekharan and N. Manoj, *New J. Chem.*, 2020, 44, 6142–6150.